

Isolated Channel Vision Transformers: From Single-Channel Pretraining to Multi-Channel Finetuning

Wenyi Lian* Joakim Lindblad Patrick Micke Nataša Sladoje
Uppsala University

<https://github.com/shermanlian/IC-ViT>

wenyi.lian@it.uu.se

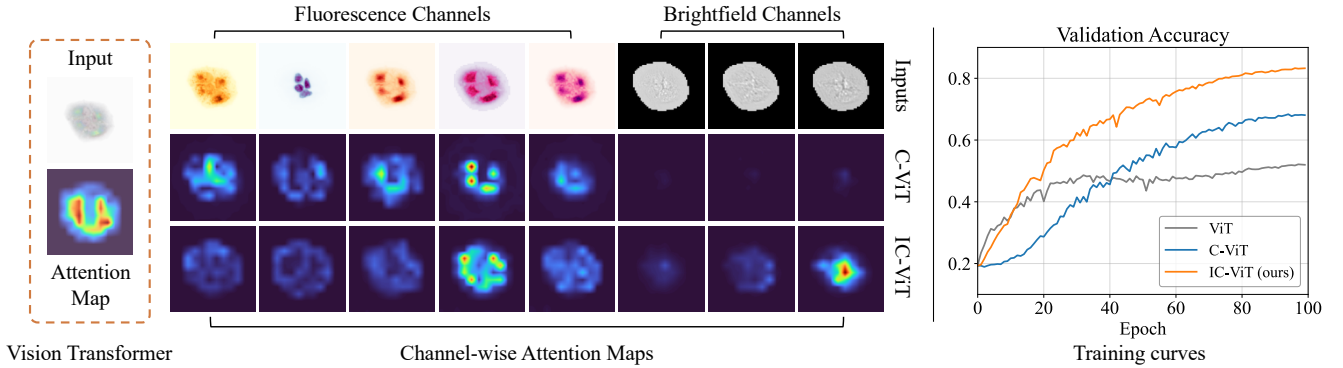


Figure 1. **Left:** Visualization of the attention maps generated from the standard Vision Transformer (ViT) [16], ChannelViT (C-ViT) [5], and the proposed Isolated Channel ViT (IC-ViT). Note that ViT compromises all channels into one patch token while ChannelViT and IC-ViT generate patch tokens for each channel individually. Our IC-ViT tends to extract information from both fluorescence and brightfield channels, while the latter is often ignored by ChannelViT. **Right:** Performance comparison on the JUMP-CP validation dataset [9].

Abstract

Vision Transformers (ViTs) have achieved remarkable success in standard RGB image processing tasks. However, applying ViTs to multi-channel imaging (MCI) data, e.g., for medical and remote sensing applications, remains a challenge. In particular, MCI data often consist of layers acquired from different modalities. Directly training ViTs on such data can obscure complementary information and impair the performance. In this paper, we introduce a simple yet effective pretraining framework for large-scale MCI datasets. Our method, named *Isolated Channel ViT (IC-ViT)*, patchifies image channels individually and thereby enables pretraining for multimodal multi-channel tasks. We show that this channel-wise patchifying is a key technique for MCI processing. More importantly, one can pretrain the IC-ViT on single channels and finetune it on downstream multi-channel datasets. This pretraining framework captures dependencies between patches as well as channels and produces robust feature representation. Experiments

on various tasks and benchmarks, including JUMP-CP and CHAMMI for cell microscopy imaging, and So2Sat-LCZ42 for satellite imaging, show that the proposed IC-ViT delivers 4–14 percentage points of performance improvement over existing channel-adaptive approaches. Further, its efficient training makes it a suitable candidate for large-scale pretraining of foundation models on heterogeneous data.

1. Introduction

Self-supervised learning (SSL) of Vision Transformers (ViTs), e.g., by DINO [8] and DINOv2 [33], has demonstrated superior advantages [2, 33, 45] in facilitating learning of generalizable representations. Application of a SSL model typically consists of two stages: (1) pretraining on large-scale unlabeled data, to learn general representations; (2) fine-tuning on downstream datasets to effectively solve real and specific tasks [17, 46]. However, an observed limitation of ViT-based SSL models is that they, in both stages, take as input images of a certain type and do not accommodate images of multi-modalities and with a varying number

*Corresponding author

of channels, e.g., multi-channel imaging (MCI) [7].

MCI is increasingly important in domains such as medical imaging and remote sensing, as it offers to capture more comprehensive and detailed information compared to traditional gray or RGB imaging [7, 15, 44]. Examples include magnetic resonance imaging, multiplex immunohistochemistry, and multichannel microscopy techniques that enable simultaneous detection of multiple biomarkers in a tissue section [3]. The channel diversity of MCI techniques and datasets imposes a challenge in developing effective method to capture information from different modalities of each channel [26, 28, 30, 32]. A commonly used approach to tackle this challenge is to finetune large-scale pretrained ViTs to MCI data. The patch embedding layer is reconstructed to fit the varying number of channels. However, directly transferring ViTs pretrained on RGB-data to multimodality MCI datasets may lead to embedding mismatch [14], resulting in suboptimal utilization of the multi-channel information [46].

Some recent works thus turn the focus on exploring modification of the ViT architecture to better accommodate multi-channel images [5, 6, 13, 34, 36]. These approaches, usually called *channel-adaptive* ViTs, propose to extract embeddings for each input channel and then concatenate them into a sequence to retain distinct information from all channels. However, the expansion of vector sequence substantially increases the computational cost and prolongs training time, posing a critical challenge in large-scale self-supervised pretraining [5].

In this paper, we present a simple yet efficient SSL algorithm for MCI data pretraining. Specifically, our method, named isolated channel ViT (IC-ViT), patchifies images along channels and, in the pretraining stage, only learns representation for each channel individually. We show that the single-channel pretrained IC-ViT not only brings computational efficiency but also produces informative features for all channels. By finetuning on downstream specific tasks, the IC-ViT further learns to capture dependencies across channels and significantly improves the prediction results. As shown in Fig. 1, attention maps of an eight channel microscopy image generated by IC-ViT illustrate that our method extracts relevant information from both fluorescence and brightfield channels. The training curves also exhibit a superior performance of the proposed method on the downstream classification task on JUMP-CP dataset [9]. Moreover, IC-ViT can potentially be trained on large MCI datasets with varying channels and modalities, showing a promising direction of MCI foundation models.

In summary, our key contributions are as follows:

- We present a simple yet efficient self-supervised learning algorithm for multi-channel image pretraining.
- We demonstrate the importance of channel-wise patchifying and show that pretraining ViTs on single

channels can still learn robust feature representations.

- The proposed IC-ViT handles varying-channel inputs well, enabling creating foundation models for multi-channel datasets.
- Extensive experiments and analysis on different datasets and tasks illustrate the effectiveness of the proposed method.

2. Related work

2.1. Self-supervised Learning

Self-supervised learning (SSL) has become increasingly popular due to its effectiveness in learning high-quality representations without requiring costly annotations of large-scale datasets [12, 20, 23, 25, 42]. A pioneering SSL method is SimCLR [10, 11], which effectively learns meaningful representations from unlabeled data by maximizing similarity between different augmented views of the same sample through contrastive learning. Following the success of contrastive learning on Convolutional Neural Networks (CNNs) [29], researchers have explored alternative SSL approaches that eliminate the need for explicit negative samples and adapt better to other architectures, such as ViTs [1, 4, 20]. DINO [8], is the first method to utilize self-distillation for SSL of ViTs, effectively learning representations without requiring explicit negative samples. Specifically, it adopts a teacher-student approach in which the student network is trained by minimizing differences with a teacher network. DINOv2 [33] further improves upon DINO by incorporating masked image modeling techniques into training, enhancing architecture, and leveraging larger-scale data. This resulted in more robust and generalizable visual feature learning. Masked Autoencoder (MAE) [21] is another self-supervised learning method for ViTs that does not require negative samples and learns by reconstructing heavily masked image patches.

2.2. Channel-adaptive Vision Transformers

While ViTs [16] have been highly successful, they have mainly been applied to RGB images [19, 39]. However, multi-channel imaging is finding increased use in many fields, since it captures richer information beyond traditional RGB [26, 28, 30, 32]. This has led to the development of channel-adaptive models for multi-channel data [13, 18, 36]. Recently, ClimaX [31] is presented as a variant of the ViT that employs variable tokenization and aggregation methods to process heterogeneous weather and climate data. DepthwiseViT [13] proposes to process each input channel separately using a depthwise convolution layer. The extracted features are then aggregated by averaging, forming a new representation that is then passed into the ViT backbone. ChannelViT [5] and ChAda-ViT[6] both generate patch tokens independently for each channel

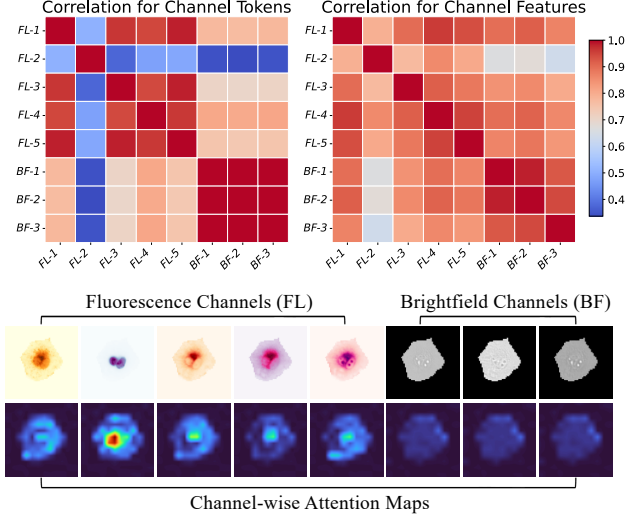


Figure 2. **Top:** Pairwise correlation of channel tokens and of channel features, for the 8 microscopy channels. **Bottom:** Visualization of a multi-channel microscopy image and its channel-wise attention maps. Here shown results are generated by applying a DINOv2 pretrained IC-ViT on a multi-channel image from JUMP-CP [9] dataset.

and incorporate learnable channel embeddings to explicitly differentiate between channels. Additionally, ChannelViT introduces Hierarchical Channel Sampling (HCS) during training to improve training efficiency. Building upon ChannelViT, DiChaViT [34] further enhances feature diversity by adopting a Diverse Channel Sampling (DCS) strategy. DCS selectively samples less similar channels, reducing redundancy and mitigating over-similarity in channel representations. However, existing channel-adaptive methods suffer from high computational costs due to channel-to-sequence expansion.

3. Method

Multi-channel images often consist of layers acquired by different procedures or from different modalities. An example of an eight-channel image, showing channels of fluorescence and brightfield microscopy, is presented at the bottom of Fig. 2. These layers typically exhibit distinct and complementary information that need to be combined to facilitate downstream task analysis. In this section, we focus on the ViT architecture and study *why* channel-wise patchifying matters for multi-channel images and explore *how* to efficiently extract informative features across channels.

3.1. Channel-wise Patchifying ViT

Image patchifying is an important step in all vision transformers which splits the 2D image $\mathbf{x} \in \mathbb{R}^{H \times W \times C}$ into N patches $\mathbf{x}_n \in \mathbb{R}^{P^2 \times C}$, where P is the patch size and $N =$

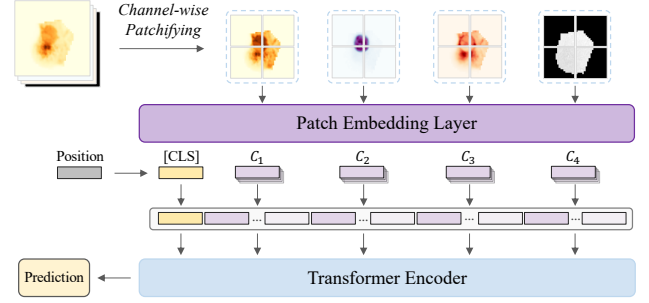


Figure 3. Illustration of the channel-wise patchifying in IC-ViT. We patchify each channel individually and embed all patches into a vector (and add position and ‘[CLS]’ embeddings) as the final input to the transformer. C_i means embeddings of the i th channel.

HW/P^2 . ViT then maps each image patch into an embedding using a learnable linear projection $\mathbf{W} \in \mathbb{R}^{P^2 C \times D}$ and concatenates all patches as a vector sequence $\mathbf{z} \in \mathbb{R}^{N \times D}$, where D is the embedding dimension. In addition, a position embedding is added to retain positional information and a learnable classification token (‘[CLS]’) embedding is inserted at the start, to serve for final prediction.

Correlation between channels Before considering the channel-wise patchifying ViT, we first study the correlation between channels in MCI data. For this purpose, we conduct an experiment to train a ViT model for each channel individually on the JUMP-CP microscopy dataset [9] using DINOv2 [33] for self-supervised feature representation learning.

The results are illustrated at the top of Fig. 2, in which we show pairwise correlations of channel tokens (image patches) and of learned channel features, for the 8 channels in an example from the JUMP-CP dataset. Note that channel tokens from fluorescence and brightfield images have a lower correlation compared to the tokens from the same modality, indicating that the two types of channels carry complementary information from different modalities. Intuitively, projecting all channels in the patch into a single embedding is similar to performing an “early fusion” in a multimodal fusion network [35], which has been shown to be ineffective for many multimodal learning tasks [22, 24, 27]. Compared to the tokens, all channel features exhibit higher pairwise correlation, which makes it easier to perform fusion without losing distinct information. The attention maps in Fig. 2 (bottom) further illustrate that the trained ViT considers both fluorescence and brightfield channels. These observations show that training ViTs on isolated channels is effective and, therefore, the channel-wise patchifying is naturally introduced to tackle the multi-channel imaging problem [5, 34].

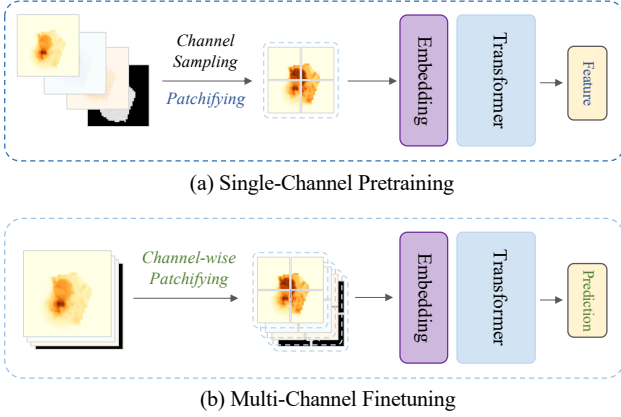


Figure 4. Overview of the (a) single-channel pretraining combined with (b) multi-channel finetuning framework. Our IC-ViT samples single channel images for efficient self-supervised pretraining and utilizes all channels in the downstream task for final prediction.

Channel-wise patchifying The main idea of channel-wise patchifying is to split the image into multiple single-channel images and patchify these images individually. The same projection layer is used for all channels. After projection, we concatenate all channel patch embeddings sequentially as the final input vector to the transformer. An overview of this approach is shown in Fig. 3. The resulting vector sequence $\tilde{\mathbf{z}} \in \mathbb{R}^{N \times C \times D}$ retains all information from each channel and is C times longer than that in the original ViT. Moreover, a learnable channel embedding is often added to indicate the spatial index of each channel, similar to the position embedding in ViT [5]. The transformer encoder can then utilize the self-attention to capture dependencies between patches as well as between channels to extract a more robust feature representation.

3.2. Efficient Multi-Channel Pretraining

We have shown the importance of channel-wise patchifying in Sec. 3.1 and also illustrated the effectiveness of feature extraction with DINOv2 pretraining in Fig. 2. However, as we mentioned before, channel-wise patchifying extends the sequence length by C times, thus increasing the computation cost quadratically with the number of channels due to the self-attention mechanism. This would largely limit the pretraining process, particularly for self-supervised algorithms like DINO [8] and DINOv2 [33] that input multiple views of the data each iteration (through augmentation) and require dual networks (as teacher and student) throughout the training.

Single-channel pretraining Training ViTs for individual channels, as described in Sec. 3.1, has empirically demonstrated potential to extract informative channel representa-

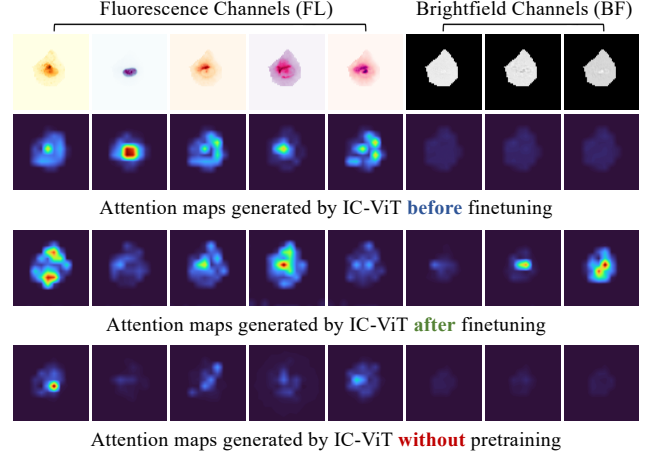


Figure 5. Attention maps on an eight-channel microscopy image generated by IC-ViT with and without fine-tuning on JUMP-CP dataset [9]. Here, “without pretraining” in the bottom row means the model is directly trained with label supervision.

tions. Since the channel-wise patchifying does not include any channel specific parameters, we can update the number of channels without additional network modification (ViT allows adaptive sequence length). The ViT pretrained on the individual channels can then be finetuned on multi-channel images for a downstream task. This approach, which we refer to as **Isolated Channel ViT (IC-ViT)**, is highly efficient for MCI pretraining and also facilitates downstream task transferring. The implementation of the framework is shown in Fig. 4. In the pretraining stage, we randomly sample one channel per image and patchify it as for a regular ViT processing of single-channel (grayscale) images. We use DINOv2 [33] for learning (individual) channel representations. During finetuning, we instead apply the channel-wise patchifying to all the channels simultaneously, to learn to utilize the global information across channels.

Fig. 5 illustrates the attention maps generated by IC-ViT with different training strategies. Apparently, all models focus more on the fluorescence modality, presumably because it contains more distinct information. The pretrained IC-ViT captures the outline feature of brightfield channels. Following the supervised finetuning relying on class-label annotations, the IC-ViT is able to utilize information from both fluorescence and brightfield channels. We also observe that directly training with label supervision (no pretraining) loses the attention of the brightfield channels, which in turn leads to inferior performance compared to the finetuned version. We provide further details in Sec. 4.

MCI foundation models Thanks to the efficient pretraining and finetuning scheme, the proposed IC-ViT can potentially be trained on large MCI datasets with varying chan-

nels and modalities. Typically, a fundamental challenge in training models on multimodal multi-channel datasets lies in the inherent difficulty of unifying image channels within the same training batch, which is a prerequisite for all existing deep learning frameworks. Two commonly used approaches are: (1) padding all images along the channel dimension, analogous to sentence padding in language models [37], and (2) conducting separate forward passes for different channel batches followed by gradient aggregation for parameter updates [34]. However, both approaches suffer from rigidity and are constrained by the variability in channel numbers. In contrast, our proposed IC-ViT solves this issue by sampling only a single channel from each image at a time, thereby ensuring channel uniformity within the batch while maintaining training efficiency.

4. Experiments

In this section we evaluate the proposed IC-ViT method on different tasks and multi-channel imaging datasets and compare with state-of-the-art channel-adaptive approaches. Details of the datasets, tasks, and implementations are described in Sec. 4.1 while results are reported in Sec. 4.2.

4.1. Datasets and Implementation

Datasets We consider three publicly available multi-channel benchmark datasets from medical and remote sensing domains including:

- *JUMP-CP* [9], a widely used benchmark for cell microscopy imaging designed to evaluate perturbation effects and learn informative representations of cellular states. This dataset has 160 perturbation in total, with each image captured across eight channels: five fluorescence and three brightfield. It includes two main tasks: perturbation detection and perturbation matching. Following previous works [5, 34], we focus on perturbation detection, aiming to identify which chemical or genetic perturbations lead to morphological changes in cells. We use the compound perturbation plate ‘BR00116991’, which comprises 127K training images, 45K validation images, and 45K test images.
- *CHAMMI* [13], a microscopy benchmark for channel-invariant models which combines three multi-channel imaging datasets with varying channel counts: WTC-11 hiPSC (WTC-11, 3 channels, 65K images) [41], Human Protein Atlas (HPA, 4 channels, 67K images) [40], and Cell Painting (CP, 5 channels, 88K images) [43]. This evaluation framework includes 9 biologically relevant tasks. In this study, the overall performance is measured by their defined *CHAMMI Performance Score* which evaluates the feature representation on domain generalization tasks [13, 34].

- *So2Sat-LCZ42* [47], a diverse remote sensing dataset comprising high-resolution multi-spectral images from 42 cities worldwide, annotated with 17 labels reflecting various local climate zones (LCZ). This dataset offers a rich blend of synthetic aperture radar (SAR) and optical information with 8 Sentinel-1 channels and 10 Sentinel-2 channels. In our experiments of LCZ prediction, we use the second version of this dataset (referred to as the ‘city split’ [5, 34]), which consists of 352K training images, 24K validation images, and 24K test images.

Training details The training of our IC-ViT consists of two stages: pretraining and fine-tuning. We adopt DI-NOv2 [33] for self-supervised pretraining which does not require any annotations. The small version of Vision Transformer (ViT-S/16) is used as the backbone. The patch size is set to 16 for all tasks except the So2Sat, in which we lower the patch size to 8, to better capture high-resolution satellite details and align with previous works [5, 34]. We apply the proposed single-channel sampling strategy for pretraining in all tasks. Note that only the training data are utilized during the pretraining phase. To fine-tune our model, and to ensure a fair comparison, we follow the same framework settings as ChannelViT [5] and DiCha-ViT [34]. More specifically, we optimize our models using cross-entropy loss on JUMP-CP and So2Sat, and using a proxy loss [38] for CHAMMI¹.

Evaluation For both JUMP-CP and So2Sat, the epoch achieving the highest validation accuracy is chosen, and the test set performance of that checkpoint is reported as the final top-1 accuracy. For CHAMMI, we use the final epoch’s checkpoint and report the macro-average F1 score computed using a linear classifier for each task. We also present the score averaged from WTC and HPA tasks as an overall performance score.

Comparison approaches We compare the proposed IC-ViT to the following state-of-the-art channel-adaptive approaches: DepthwiseViT [13], TemplateMixingViT [36], HyperNetViT [18], ChAda-ViT [6], ChannelViT [5], and DiChaViT [34]. Considering that ChannelViT uses exactly the same architecture as our IC-ViT, we regard it as the main reference method. Following [34], the HCS [5] is applied to all models to ensure a fair comparison.

4.2. Results

The quantitative results are reported in Table 1. For the JUMP-CP and So2Sat datasets, our evaluations cover two

¹For more details on datasets, training settings, codes, and additional results, please refer to the supplementary materials

Model	CHAMMI [13]			JUMP-CP [9]		So2Sat [47]	
	WTC	HPA	Avg F1-score	Full	Partial	Full	Partial
DepthwiseViT [13]	50.35	71.52	60.94	49.86	44.98	60.41	43.41
TemplateMixingViT [36]	49.51	64.52	57.02	52.48	43.85	55.86	37.28
HyperNetViT [18]	45.17	63.90	54.54	47.07	42.43	60.73	41.88
ChAda-ViT [6]	67.08	60.67	63.88	65.03	42.15	56.98	12.38
ChannelViT [5]	67.66	62.14	64.90	67.51	56.49	61.03	46.16
DiChaViT [34]	73.36	63.35	68.36	69.19	57.98	63.36	47.76
IC-ViT (Ours)	74.53	70.55	72.54	83.41	65.88	67.41	48.55

Table 1. Comparison of method performance on test sets of three multi-modal and multi-channel image benchmarks: CHAMMI, JUMP-CP, and So2Sat. Best scores are shown in **bold**. For the CHAMMI dataset, the overall F1 score is calculated by averaging the “WTC” and “HP” subsets, consistent with the original paper. JUMP-CP and So2Sat is evaluated using top-1 accuracy. “Full” means all channels are used at test time, whereas “Partial” refers to using only a subset (fluorescence channels for JUMP-CP and Sentinel-1 channels for So2Sat).

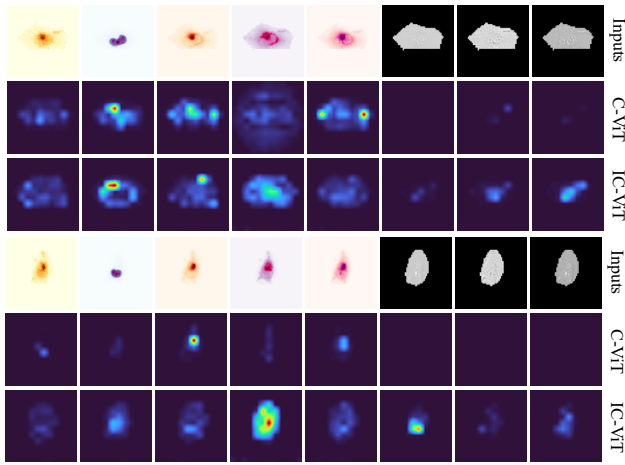


Figure 6. Comparison of channel-wise attention maps generated by ChannelViT (C-ViT) and our IC-ViT on JUMP-CP dataset. IC-ViT better exploits information available in the channels.

practical scenarios: (1) training and testing with all channels (denoted as “Full”); and (2) training with all, but testing only with a partial set of channels (denoted as “Partial”), simulating situations where only one modality is available at inference (the fluorescence channels for JUMP-CP and the Sentinel-1 channels for So2Sat). We observe that the proposed IC-ViT consistently outperforms other approaches across most tasks and datasets. Particularly, IC-ViT improves accuracy compared to the reference model ChannelViT with about 14% points for full channel evaluation and 8% points for partial channel evaluation on the JUMP-CP dataset, demonstrating the effectiveness and robustness of the proposed framework. An attention map comparison between ChannelViT and IC-ViT is provided in Fig. 6. It indicates the efficient usage of available information by the IC-ViT model. Our method achieves a 4.18% points improvement in overall F1-score compared

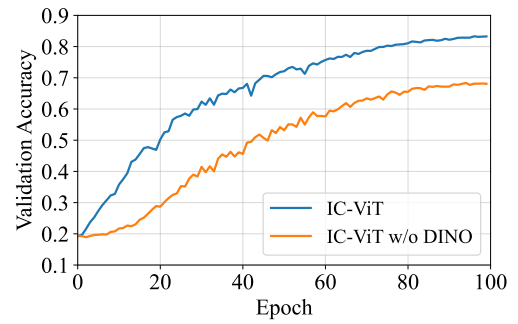


Figure 7. Validation accuracy across epochs on the JUMP-CP dataset: IC-ViT vs. IC-ViT without DINOv2 pretraining on the JUMP-CP dataset.

to the second-best method, DiChaViT, on the CHAMMI benchmark, further demonstrating the strong ability of robust feature representation learning and generalization.

5. Analysis and Discussion

In this section we present several ablation experiments to analyze the key properties of the proposed framework.

5.1. Effectiveness of Self-Supervised Learning

We evaluate the importance of self-supervised learning for our method by comparing models trained with and without DINOv2 pretraining on the JUMP-CP dataset. As presented in Fig. 7, the model with DINOv2 pretraining outperforms its supervised-only counterpart by a substantial margin in downstream validation accuracy, clearly demonstrating the advantage of incorporating self-supervised representations.

5.2. Pretraining Time Efficiency

A major limitation of channel-adaptive approaches is the increased computational cost caused by expanding the channel dimension into the sequence length. Here, we report

Model (S/16)	#Channels	Batch size	Time (hh:mm)
ViT	8	128	21:56
IC-ViT w/ HCS	—	16	86:28
IC-ViT	8	16	126:53
IC-ViT	5	32	56:03
IC-ViT	3	64	28:53
IC-ViT (proposed)	1	128	09:16

Table 2. Pretraining time (in hours:minutes) across different models and channel configurations on the JUMP-CP training set ($\sim 127K$ images). All experiments are run for 100 epochs of DINOv2 pretraining on four NVIDIA A100-SXM4-80GB GPUs, employing a ViT-S/16 backbone (22M parameters). Batch sizes are adjusted based on the available memory. The number of channels in ‘IC-ViT w/ HCS’ is dynamically selected (denoted with ‘—’).

#Channels	1	3	5
Accuracy	83.25	79.44	78.09

Table 3. Validation accuracy (%) for different counts of channels randomly selected during the pretraining.

a comparison of pretraining time for ViT and variants of the IC-ViT on the JUMP-CP training set for 100 epochs. Table 2 shows that pretraining the IC-ViT on all channels without any sampling strategy [5] on the JUMP-CP dataset requires 5 days and 6 hours on four 80GB A100 GPUs. Although using Hierarchical Channel Sampling (HCS) during DINO pretraining can shorten this duration to 3 days and 14 hours, it is observed to introduce instability to the self-distillation objective [5].

For the proposed IC-ViT, only one channel is selected per image at each iteration, which significantly reduces the pretraining time to 9 hours, indicating the potential of our method for scaling to large-scale datasets. We test model pretraining using different number of (randomly selected) channels, as shown in Table 2. We observe that pretraining with 3 channels takes roughly 3 times longer than with a single channel, while using 5 channels demands nearly 6 times the duration. These models are then fine-tuned on the JUMP-CP dataset for task-specific evaluation. In Table 3, we report the validation accuracy for pretraining with different number of channels. Somewhat surprisingly, including additional randomly selected channels does not surpass the single-channel setup, confirming the efficiency of our proposed idea.

5.3. Effectiveness of Channel-wise Patchifying

The standard ViT [16] treats all patches uniformly without differentiating among input channels, thereby neglecting the potentially independent semantic content carried by each channel/modality [5]. In this study, we first pre-train ViT, and our IC-ViT using DINOv2 on the JUMP-

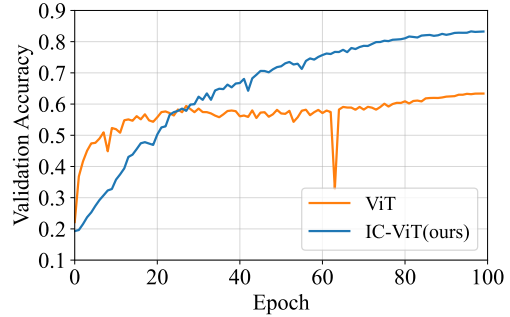


Figure 8. Performance comparison of the proposed IC-ViT and ViT: both are pretrained and finetuned on the JUMP-CP dataset.

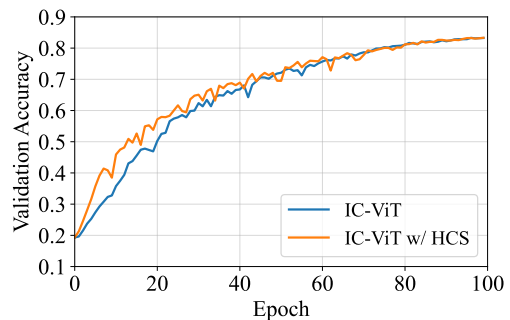


Figure 9. Training curves of IC-ViT and its variant i.e. pretraining IC-ViT on all channels with the HCS strategy [5].

CP dataset, and subsequently fine-tune both models on the downstream task from the same dataset. The corresponding training curves are illustrated in Fig. 8. While the pretrained ViT initially achieves higher accuracy, its performance stagnates after approximately 10 epochs. In contrast, our IC-ViT continues to steadily improve, highlighting the effectiveness of the channel-wise patchifying.

In addition, we further explore a variant of the IC-ViT: pretraining ViT on all channels but adding the HCS strategy [5]. This variant choose to sample a fixed number of channels at each iteration, providing broader exposure to channel information per iteration compared to our method. However, as can be observed from Fig. 9, although this variant achieves higher accuracy initially, its advantage diminishes with increased training, leading to a comparable final performance to our method. We note that pretraining 8-channel IC-ViT with HCS takes more than nine times longer time than our IC-ViT, as reported in Table 2, further highlighting the efficiency of our method.

5.4. Robustness Evaluation on Channel Subsets

Table 1 demonstrates that our approach outperforms others when an entire modality is absent at inference, indicating a potential for handling images with missing channels.

#channels	#comb.	ViT	ChannelViT	IC-ViT (Ours)
8	1	56.87	68.09	83.41
7	8	49.35 \pm 09.38	61.02 \pm 09.78	79.72 \pm 06.87
6	28	42.38 \pm 10.64	53.45 \pm 12.40	72.42 \pm 10.11
5	56	35.78 \pm 10.18	45.50 \pm 13.23	63.40 \pm 12.31
4	70	29.84 \pm 08.32	37.37 \pm 12.25	52.56 \pm 13.10
3	56	24.94 \pm 05.43	29.68 \pm 09.22	40.33 \pm 11.71
2	28	21.54 \pm 02.37	23.77 \pm 04.89	28.80 \pm 07.45
1	8	19.92 \pm 00.51	20.85 \pm 01.64	21.84 \pm 02.54

Table 4. Test accuracy on JUMP-CP dataset [9]. Here, we evaluate the model with different number of channels and all possible channel combinations during inference. ‘#comb.’ denotes the number of $\binom{8}{k}$ combinations. Mean and standard deviation are reported (when #comb>1). For any number of channels, our proposed IC-ViT delivers the best performance. The results of ViT and ChannelViT are reported from their original paper [5].

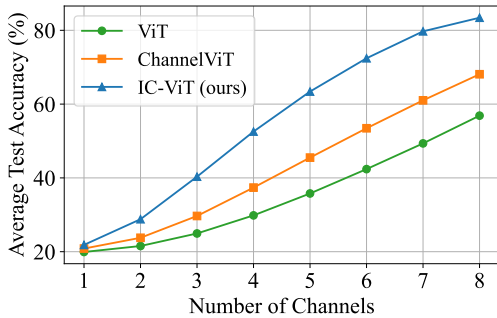


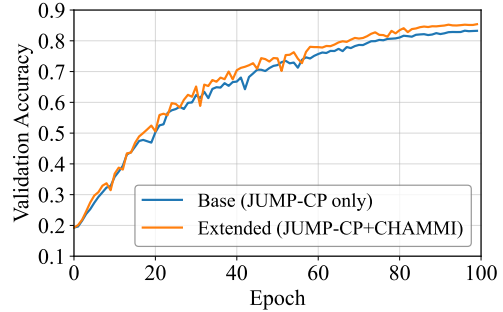
Figure 10. Average test accuracy (%) across all combinations of channels, for each given number of inference input channels on the JUMP-CP dataset.

Here, we further extend the evaluation to random channel-missing scenarios by analyzing test accuracy on the JUMP-CP dataset when various subsets of channels are removed during inference. All possible channel combinations are evaluated, and Table 4 reports the mean and standard deviation across these combinations for different methods.

As illustrated in Table 4 and Fig. 10, our method consistently exhibits higher average accuracy across various combinations of input channels, indicating strong robustness to partial or missing channel inputs. Moreover, the steady accuracy improvement with more available channels, as depicted in Fig. 10, further suggests that our single channel sampling strategy effectively captures and fuses independent semantic information from each channel, enhancing the diversity and informativeness of extracted features.

5.5. Pretraining with Extended Datasets

As mentioned in Sec. 3.2, IC-ViT potentially can be used for MCI foundation models, extending the training data with more multi-channel images. To evaluate the ability to han-



(a) Learning curves

	Validation acc.	Test acc.
JUMP-CP	83.25	83.41
JUMP-CP+CHAMMI	85.40	85.69

(b) Quantitative results

Figure 11. Multi-Dataset pretraining evaluation. (a) Validation accuracy curves for the baseline model (pretrained solely on JUMP-CP) and the extended model (pretrained on both JUMP-CP and CHAMMI). The extended pretraining generally results in higher accuracy throughout training. (b) Test accuracy at the epoch of highest validation accuracy. Best results in **bold**.

dle variable-channel inputs, we compare the baseline IC-ViT model pretrained solely on the JUMP-CP dataset, with an extended version pretrained on both the JUMP-CP and CHAMMI datasets. Both pretrained models are then finetuned on the JUMP-CP dataset under the same experimental settings. As shown in Fig. 11 (a), the larger-scale pretrained model generally leads to higher validation accuracy across most training epochs. Moreover, as summarized in Fig. 11 (b), using additional data achieves an improvement of over 2% points in both validation and test accuracies. Given that CHAMMI is a variable-channel dataset itself, the overall 4% performance improvement achieved by our method (see Tab. 1) also indicates its potential for effective pretraining on images with varying numbers of channels.

6. Conclusion

In this study, we address the problem of channel-adaptive learning on multi-channel imaging (MCI) data and present an efficient framework to pretrain and finetune ViTs on MCI datasets. The proposed Isolated Channel Vision Transformer (IC-ViT) patchifies images per individual channel and accommodates varying-channel datasets. We show that IC-ViT effectively learns informative channel representation. Subsequent finetuning on downstream multi-channel tasks efficiently captures complementary information from different channels and modalities. Being compute-efficient, training of IC-ViT can be performed on large-scale datasets, enabling establishing MCI foundation models. We per-

form extensive experiments on various tasks and datasets, demonstrating the effectiveness of the proposed IC-ViT. In our future work, we plan to scale the model to larger datasets and specific downstream tasks.

Acknowledgement

The computations and data handling were enabled by resources provided by Chalmers e-Commons at Chalmers.

References

- [1] Sara Atito, Muhammad Awais, and Josef Kittler. Sit: Self-supervised vision transformer. *arXiv preprint arXiv:2104.03602*, 2021. 2
- [2] Muhammad Awais, Muzammal Naseer, Salman Khan, Rao Muhammad Anwer, Hisham Cholakkal, Mubarak Shah, Ming-Hsuan Yang, and Fahad Shahbaz Khan. Foundation models defining a new era in vision: a survey and outlook. *IEEE TPAMI*, 2025. 1
- [3] Max Backman, Carina Strell, Amanda Lindberg, Johanna SM Mattsson, Hedvig Elfving, Hans Brunnström, Aine O'Reilly, Martina Bosic, Miklos Gulyas, Johan Isaksson, et al. Spatial immunophenotyping of the tumour microenvironment in non-small cell lung cancer. *European Journal of Cancer*, 185:40–52, 2023. 2
- [4] Hangbo Bao, Li Dong, Songhao Piao, and Furu Wei. BEiT: BERT pre-training of image transformers. In *ICLR*, 2022. 2
- [5] Yujia Bao, Srinivasan Sivanandan, and Theofanis Karaletsos. Channel vision transformers: An image is worth 1 x 16 x 16 words. In *ICLR*, 2024. 1, 2, 3, 4, 5, 6, 7, 8
- [6] Nicolas Bourrieux, Ihab Bendidi, Ethan Cohen, Gabriel Watkinson, Maxime Sanchez, Guillaume Bollot, and Auguste Genovesio. ChAda-ViT: Channel adaptive attention for joint representation learning of heterogeneous microscopy images. In *CVPR*, pages 11556–11565, 2024. 2, 5, 6
- [7] Lei Cai, Jingyang Gao, and Di Zhao. A review of the application of deep learning in medical image classification and segmentation. *Annals of Translational Medicine*, 8(11):713, 2020. 2
- [8] Mathilde Caron, Hugo Touvron, Ishan Misra, Hervé Jégou, Julien Mairal, Piotr Bojanowski, and Armand Joulin. Emerging properties in self-supervised vision transformers. In *ICCV*, pages 9650–9660, 2021. 1, 2, 4
- [9] Srinivas Niranj Chandrasekaran, Beth A Cimini, Amy Goodale, Lisa Miller, Maria Kost-Alimova, Nasim Jamali, John G Doench, Briana Fritchman, Adam Skepner, Michelle Melanson, et al. Three million images and morphological profiles of cells treated with matched chemical and genetic perturbations. *Nature Methods*, 21(6):1114–1121, 2024. 1, 2, 3, 4, 5, 6, 8
- [10] Ting Chen, Simon Kornblith, Mohammad Norouzi, and Geoffrey Hinton. A simple framework for contrastive learning of visual representations. In *International Conference on Machine Learning*, pages 1597–1607. PmLR, 2020. 2
- [11] Ting Chen, Simon Kornblith, Kevin Swersky, Mohammad Norouzi, and Geoffrey E Hinton. Big self-supervised models are strong semi-supervised learners. *NeurIPS*, 33:22243–22255, 2020. 2
- [12] Xinlei Chen, Haoqi Fan, Ross Girshick, and Kaiming He. Improved baselines with momentum contrastive learning. *arXiv preprint arXiv:2003.04297*, 2020. 2
- [13] Zitong Sam Chen, Chau Pham, Siqi Wang, Michael Doron, Nikita Moshkov, Bryan Plummer, and Juan C Caicedo. CHAMMI: A benchmark for channel-adaptive models in microscopy imaging. *NeurIPS*, 36:19700–19713, 2023. 2, 5, 6
- [14] Aloïs de La Comble and Ken Prepin. Efficient transfer learning for multi-channel convolutional neural networks. In *2021 17th International Conference on Machine Vision and Applications (MVA)*, pages 1–6. IEEE, 2021. 2
- [15] Ivica Dimitrovski, Ivan Kitanovski, Dragi Koccev, and Nikola Simidjievski. Current trends in deep learning for earth observation: An open-source benchmark arena for image classification. *ISPRS Journal of Photogrammetry and Remote Sensing*, 197:18–35, 2023. 2
- [16] Alexey Dosovitskiy, Lucas Beyer, Alexander Kolesnikov, Dirk Weissenborn, Xiaohua Zhai, Thomas Unterthiner, Mostafa Dehghani, Matthias Minderer, Georg Heigold, Sylvain Gelly, Jakob Uszkoreit, and Neil Houlsby. An image is worth 16x16 words: Transformers for image recognition at scale. In *ICLR*, 2021. 1, 2, 7
- [17] Linus Ericsson, Henry Gouk, Chen Change Loy, and Timothy M Hospedales. Self-supervised representation learning: Introduction, advances, and challenges. *IEEE Signal Processing Magazine*, 39(3):42–62, 2022. 1
- [18] David Ha, Andrew M. Dai, and Quoc V. Le. Hypernetworks. In *ICLR*, 2017. 2, 5, 6
- [19] Kai Han, Yunhe Wang, Hanting Chen, Xinghao Chen, Jianyuan Guo, Zhenhua Liu, Yehui Tang, An Xiao, Chun-jing Xu, Yixing Xu, et al. A survey on vision transformer. *IEEE TPAMI*, 45(1):87–110, 2022. 2
- [20] Kaiming He, Haoqi Fan, Yuxin Wu, Saining Xie, and Ross B. Girshick. Momentum contrast for unsupervised visual representation learning. *CVPR*, pages 9726–9735, 2019. 2
- [21] Kaiming He, Xinlei Chen, Saining Xie, Yanghao Li, Piotr Dollár, and Ross Girshick. Masked autoencoders are scalable vision learners. In *CVPR*, pages 15979–15988, 2022. 2
- [22] Xiaoyu He, Yong Wang, Shuang Zhao, and Xiang Chen. Co-attention fusion network for multimodal skin cancer diagnosis. *Pattern Recognition*, 133:108990, 2023. 3
- [23] Dan Hendrycks, Mantas Mazeika, Saurav Kadavath, and Dawn Song. Using self-supervised learning can improve model robustness and uncertainty. *NeurIPS*, 32, 2019. 2
- [24] Hamid Reza Vaezi Joze, Amirreza Shaban, Michael L Iuz-zolino, and Kazuhito Koishida. Mmtm: Multimodal transfer module for cnn fusion. In *CVPR*, pages 13289–13299, 2020. 3
- [25] Rayan Krishnan, Pranav Rajpurkar, and Eric J Topol. Self-supervised learning in medicine and healthcare. *Nature Biomedical Engineering*, 6(12):1346–1352, 2022. 2

- [26] Jae-Hyeok Lee, Sangmin S Lee, Hak Gu Kim, Sa-Kwang Song, Seongchan Kim, and Yong Man Ro. Mscip net: Multichannel satellite image prediction via deep neural network. *IEEE Transactions on Geoscience and Remote Sensing*, 58(3):2212–2224, 2019. 2
- [27] Wenyi Lian, Joakim Lindblad, Christina Runow Stark, Jan-Michaél Hirsch, and Nataša Sladoje. Let it shine: Auto-fluorescence of papanicolaou-stain improves ai-based cytological oral cancer detection. *Computers in Biology and Medicine*, 185:109498, 2025. 3
- [28] Mingxia Liu, Jun Zhang, Ehsan Adeli, and Dinggang Shen. Deep multi-task multi-channel learning for joint classification and regression of brain status. In *International Conference on Medical Image Computing and Computer-Assisted Intervention*, pages 3–11. Springer, 2017. 2
- [29] Pavan C Madhusudana, Neil Birkbeck, Yilin Wang, Balu Adsumilli, and Alan C Bovik. Image quality assessment using contrastive learning. *IEEE TIP*, 31:4149–4161, 2022. 2
- [30] Sampa Misra, Seungwan Jeon, Seiyon Lee, Ravi Managuli, In-Su Jang, and Chulhong Kim. Multi-channel transfer learning of chest x-ray images for screening of covid-19. *Electronics*, 9(9):1388, 2020. 2
- [31] Tung Nguyen, Johannes Brandstetter, Ashish Kapoor, Jayesh K Gupta, and Aditya Grover. ClimaX: A foundation model for weather and climate. In *Proc. of the 40th International Conference on Machine Learning*, pages 25904–25938. PMLR, 2023. 2
- [32] Dong Nie, Junfeng Lu, Han Zhang, Ehsan Adeli, Jun Wang, Zhengda Yu, LuYan Liu, Qian Wang, Jinsong Wu, and Dinggang Shen. Multi-channel 3d deep feature learning for survival time prediction of brain tumor patients using multimodal neuroimages. *Scientific Reports*, 9(1):1103, 2019. 2
- [33] Maxime Oquab, Timothée Darcet, Théo Moutakanni, Huy V. Vo, Marc Szafraniec, Vasil Khalidov, Pierre Fernandez, Daniel HAZIZA, Francisco Massa, Alaaeldin El-Nouby, Mido Assran, Nicolas Ballas, Wojciech Galuba, Russell Howes, Po-Yao Huang, Shang-Wen Li, Ishan Misra, Michael Rabbat, Vasu Sharma, Gabriel Synnaeve, Hu Xu, Herve Jegou, Julien Mairal, Patrick Labatut, Armand Joulin, and Piotr Bojanowski. DINOv2: Learning robust visual features without supervision. *Transactions on Machine Learning Research*, 2024. Featured Certification. 1, 2, 3, 4, 5
- [34] Chau Pham and Bryan Plummer. Enhancing feature diversity boosts channel-adaptive vision transformers. In *NeurIPS*, pages 89782–89805. Curran Associates, Inc., 2024. 2, 3, 5, 6
- [35] Dhanesh Ramachandram and Graham W Taylor. Deep multimodal learning: A survey on recent advances and trends. *IEEE Signal Processing Magazine*, 34(6):96–108, 2017. 3
- [36] Pedro Savarese and Michael Maire. Learning implicitly recurrent CNNs through parameter sharing. In *ICLR*, 2019. 2, 5, 6
- [37] Ilya Sutskever, Oriol Vinyals, and Quoc V Le. Sequence to sequence learning with neural networks. *Advances in neural information processing systems*, 27:3104–3112, 2014. 5
- [38] Eu Wern Teh, Terrance DeVries, and Graham W Taylor. Proxynca++: Revisiting and revitalizing proxy neighborhood component analysis. In *ECCV*, pages 448–464. Springer, 2020. 5
- [39] Hans Thisanake, Chamli Deshan, Kavindu Chamith, Sachith Seneviratne, Rajith Vidanaarachchi, and Damayanthi Herath. Semantic segmentation using vision transformers: A survey. *Engineering Applications of Artificial Intelligence*, 126:106669, 2023. 2
- [40] Peter J Thul, Lovisa Åkesson, Mikaela Wiking, Diana Mahdessian, Aikaterini Geladaki, Hammou Ait Blal, Tove Alm, Anna Asplund, Lars Björk, Lisa M Breckels, et al. A subcellular map of the human proteome. *Science*, 356(6340):eaal3321, 2017. 5
- [41] Matheus P Viana, Jianxu Chen, Theo A Knijnenburg, Ritvik Vasani, Calysta Yan, Joy E Arakaki, Matte Bailey, Ben Berry, Antoine Borensztein, Eva M Brown, et al. Integrated intracellular organization and its variations in human ips cells. *Nature*, 613(7943):345–354, 2023. 5
- [42] Yi Wang, Conrad M Albrecht, Nassim Ait Ali Braham, Lichao Mou, and Xiao Xiang Zhu. Self-supervised learning in remote sensing: A review. *IEEE Geoscience and Remote Sensing Magazine*, 10(4):213–247, 2022. 2
- [43] Gregory P Way, Ted Natoli, Adeniyi Adeboye, Lev Litichevskiy, Andrew Yang, Xiaodong Lu, Juan C Caicedo, Beth A Cimini, Kyle Karhohs, David J Logan, et al. Morphology and gene expression profiling provide complementary information for mapping cell state. *Cell Systems*, 13(11):911–923, 2022. 5
- [44] Di Wu, Lionel Pigou, Pieter-Jan Kindermans, Nam Do-Hoang Le, Ling Shao, Joni Dambre, and Jean-Marc Odobez. Deep dynamic neural networks for multimodal gesture segmentation and recognition. *IEEE TPAMI*, 38(8):1583–1597, 2016. 2
- [45] Hanwen Xu, Naoto Usuyama, Jaspreet Bagga, Sheng Zhang, Rajesh Rao, Tristan Naumann, Cliff Wong, Zelalem Gero, Javier González, Yu Gu, et al. A whole-slide foundation model for digital pathology from real-world data. *Nature*, 630(8015):181–188, 2024. 1
- [46] Ce Zhou, Qian Li, Chen Li, Jun Yu, Yixin Liu, Guangjing Wang, Kai Zhang, Cheng Ji, Qiben Yan, Lifang He, et al. A comprehensive survey on pretrained foundation models: A history from bert to chatgpt. *International Journal of Machine Learning and Cybernetics*, pages 1–65, 2024. 1, 2
- [47] XiaoXiang Zhu, Jingliang Hu, Chunping Qiu, Yilei Shi, Jian Kang, Lichao Mou, Hossein Bagheri, Matthias Haberle, Yuansheng Hua, Rong Huang, Lloyd Hughes, Hao Li, Yao Sun, Guichen Zhang, Shiyao Han, Michael Schmitt, and Yuanyuan Wang. So2sat lc42: A benchmark data set for the classification of global local climate zones [software and data sets]. *IEEE Geoscience and Remote Sensing Magazine*, 8(3):76–89, 2020. 5, 6